Journal of Engineering Physics and Thermophysics, Vol. 75, No. 5, 2002

CALCULATION OF NONSTATIONARY FLOW AROUND A CIRCULAR CYLINDER WITHIN THE FRAMEWORK OF MULTIBLOCK COMPUTATIONAL TECHNOLOGIES

S. A. Isaev,[a] **A. G. Sudakov,**[a]
A. E. Usachov,[b] **and V. B. Kharchenko**[a]

UDC 532.517.2

A methodological numerical investigation of nonstationary flow of an incompressible viscous fluid around a circular cylinder has been carried out within the framework of the multiblock approach on a set of intersecting rectangular and cylindrical grids.

1. The problem of nonstationary flow around a cylinder is one of the best known problems, which has long been used in the practice of testing computational algorithms to solve Navier–Stokes equations. Even in 1964, J. Fromm [1] demonstrated the calculated Karman vortex street behind a cylinder having a square cross section. It should be noted that similarly to the numerical modeling of circulation flow of an incompressible fluid in a square cavity with a mobile cover (see, for example, [2]), the nonstationary Navier–Stokes equations written in transformed variables vorticity–current function were solved at the initial stage. The use of such a simplified approach is explained by the economy of computational resources.

Subsequently, in the 1980s, the computational procedures for solution of the nonstationary Navier–Stokes equations in natural variables velocity components–pressure on monoblock grids were developed (see [3, 4]). In the 1990s, much attention was given to multiblock algorithms and to adaptive and nonstructurized grids [5]. And the methods of solving the equations on multiblock grids with a component-adaptive interface have found the widest use in computational practice.

2. One promising trend in the development of the computational hydrodynamics of recent years is the development of factorized multiblock algorithms for solving the nonstationary Navier–Stokes equations on the basis of intersecting structurized grids of simple topology. The advantages of the use of such grids lie in the fact that they make it possible not only to map multiply connected regions of complex geometry on very economical grids with minimum errors caused by the angularity of the grid lines, but also to markedly improve the quality of numerical solutions by catching correctly different-scale hydrodynamic features of the flow on the corresponding narrow grids. This is particularly true for the reproduction of boundary and shear layers which are very thin at high Reynolds numbers.

The elements of multiblock computational technologies began to be developed in solving the problems of laminar stationary flow of a viscous fluid around a circular cylinder [6] and a thick profile [7] for the case where vortex cells are built into the contours of the bodies. The so-called multistage grids which make it possible to resolve the near-wall layers with a high accuracy and to simultaneously use fairly coarse grids at a large distance from the body have been tested. In the zones of intersection of the grids, the parameters have been determined using both conservative and nonconservative (linear) interpolations, and the acceptability of the latter has been shown.

The multiblock computational procedure based on multistage grids has been extended to the case of nonstationary laminar flow around a circular cylinder [8] and a rounded plane bar [9] containing vortex cells with rotating central bodies in their structures. It has also been used for analysis of the jet action on the nonstationary near wake in turbulent flow around a cylinder [10].

An extended description of the factorized multiblock algorithm for calculating nonstationary laminar flows with flow separation near bodies having a two-dimensional configuration and a detailed mapping of the flow in the near wake on a special rectangular grid are presented in [11]. The algorithm has been tested in solving the problem on the initial phase of an abrupt start of a circular cylinder in a wide range of Reynolds numbers. This phase is char-

[a]Academy of Civil Aviation, St. Petersburg, Russia; email: isaev@SI3612spb.edu; [b]State Scientific-Research Center "Central Aerohydrodynamics Institute," Moscow, Russia. Translated from Inzhenerno-Fizicheskii Zhurnal, Vol. 75, No. 5, pp. 115–121, September–October, 2002. Original article submitted March 7, 2002.

1062-0125/02/7505-1147$27.00

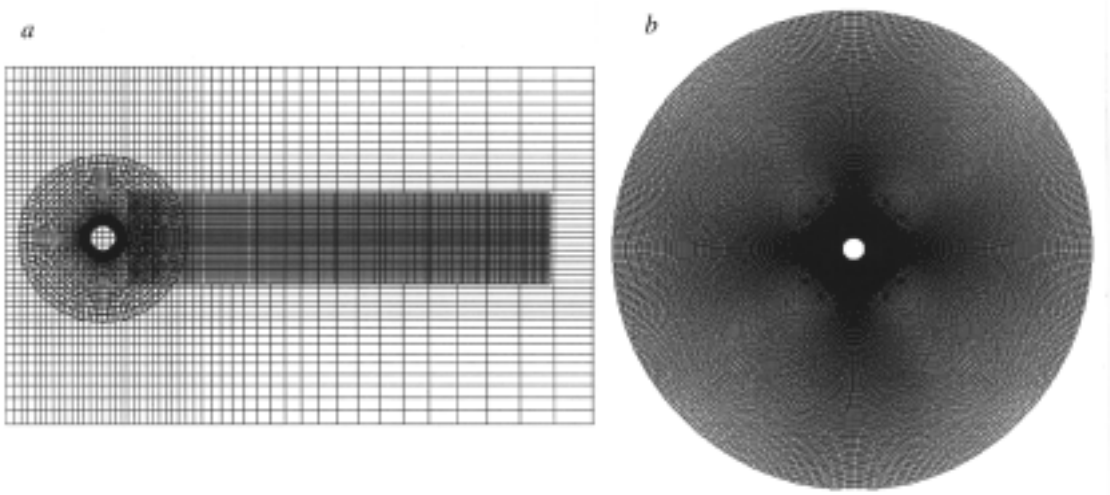

Fig. 1. Fragment of a multiblock computational grid consisting of a grid adjacent to the circular cylinder, a cylindrical grid around the cylinder, and two embedded rectangular grids, one of which is designed for description of the flow in the wake (a) and a two-stage cylindrical grid to calculate nonstationary laminar flow around a circular cylinder (b).

acterized by symmetric dynamically developing vortex structures. The aim of the present work is to numerically analyze the development of the nonstationary wake in the case of two-dimensional laminar flow around a circular cylinder within the framework of multiblock technologies with the use of grids of various types.

3. The problem of uniform flow of an incompressible viscous fluid around the body considered is solved in a two-dimensional formulation at a Reynolds number of the undisturbed flow of Re = 150. Selection of this value of the Reynolds number is explained by the fact that it falls within the range in which the model of two-dimensional flow is workable. As the comparatively recent investigations (see, for example, [12, 13]) of three-dimensional flow around a circular cylinder have shown, two-dimensional nonstationary flow exists to Re = 190.

The formulation of the problem is analogous to that presented in [8]. It is assumed that the following conditions are set at the outer boundaries of the computational region which are at a large distance from the contour of the body: the parameters of the incoming flow (they are used as the characteristic of normalization parameters) at the inlet boundary are fixed and the boundary conditions at the outlet boundary are soft. The adhesion conditions are fulfilled on the washed surfaces of the body considered.

Two variants of computational multiblock grids are selected for analysis of flow around a circular cylinder: a combination of rectangular and cylindrical grids of different scale (Fig. 1a) and a multistage cylindrical grid (Fig. 1b). The diameter of the cylinder is selected as the linear scale.

The outer rectangular region with dimensions 27×20 (Fig. 1a) contains 70×60 cells distributed nonuniformly in space. The minimum step of the grid in the neighborhood of the body is equal to 0.2. The center of the circular cylinder is positioned symmetrically relative to the upper and lower boundaries at a distance of 10 from the front boundary. The circular cylinder is surrounded by two multistage cylindrical grids. The ring grid nearest to the outer contour of the cylinder has a thickness of 0.2 and a near-wall step of 0.002. It contains 15×100 cells. The outer ring region of thickness 2 is subdivided into 20×100 cells. At a distance of 0.8 from the cylinder, there is an additional rectangular region with dimensions 13.5×3 containing 175×40 cells. The last-mentioned grid is designed for catching the features of the flow in the near and far wakes of the circular cylinder.

The methodological investigation of laminar flow around a circular cylinder also involves the calculations of two-dimensional flow on a two-stage cylindrical grid shown in Fig. 1b. The ring grid of size 0.1 with a step of 0.002 near the surface, which is nearest to the wall of the cylinder, contains 13×400 cells, and the outer ring grid of radius 10 has 200×400 cells. The radius of the outer grid varies from 10 to 20.

4. A methodological investigation of nonstationary laminar flow around a circular cylinder has been carried out earlier [8] on a multistage cylindrical grid. In the present work, we compare the results of the calculations of the

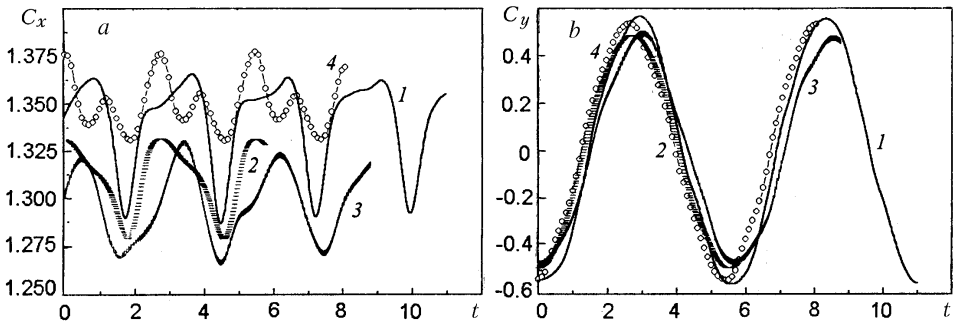

Fig. 2. Drag coefficients C_x (a) and transverse-force coefficients C_y (b) of the circular cylinder vs. time t in the self-oscillating regime of flow around it: 1–3) calculation on cylindrical grids [1) R_1 = 10; 2) 15; 3) 20]; 4) calculation on combined grids.

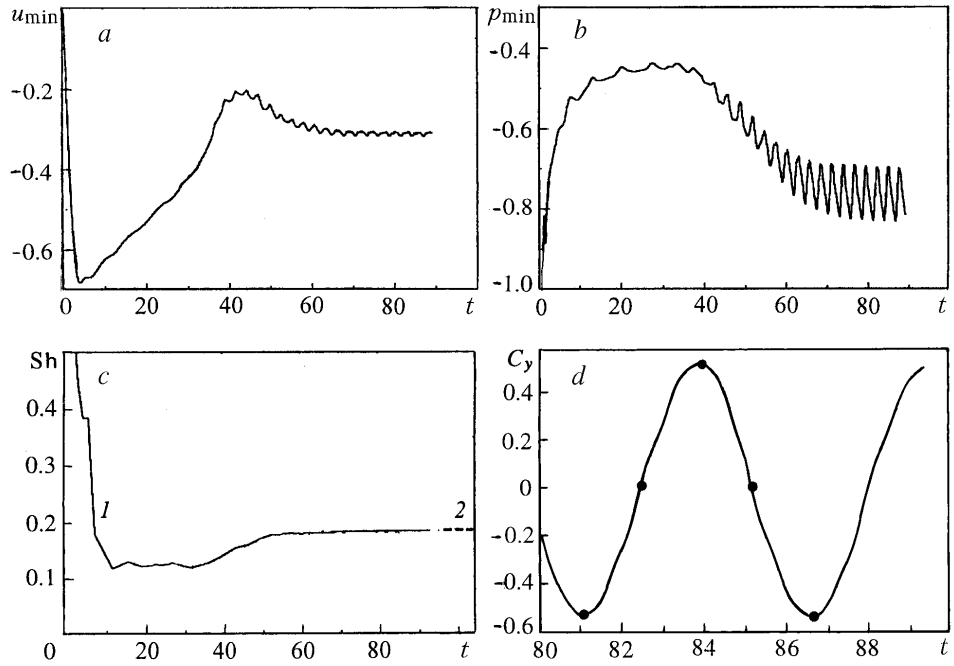

Fig. 3. Minimum values of the longitudinal velocity component u_{min} (a), static pressure p_{min} (b), and Strouhal number Sh (c) in the transient regime of laminar flow and transverse-force coefficient C_y in the self-oscillating regime of flow (d) vs. time t. Points denote the instants of time for which the patterns in Fig. 4 are constructed. Curve 1 in Fig. 3c corresponds to the calculated results and dashed line 2 corresponds to the experimental data [14–17].

integral characteristics of the cylinder on grids of different topology. Special attention is given to the evaluation of the influence of the radius R_1 of the cylindrical region of the grid on the coefficients C_x and C_y of the cylinder. We consider both the self-oscillating and transient portions of the characteristics.

In the self-oscillating regime of flow around a circular cylinder, the topology of the grid has a small influence on its integral characteristics, especially for the coefficient C_y (Fig. 2). A certain spread is observed in the drag coefficient of the cylinder as a function of the radius of the cylindrical region, and there appears a trend — the larger R_1, the lower the value of C_x. This effect can partially be explained by the blocking of the flow.

The time evolution of the integral characteristics of the circular cylinder from the beginning of motion (or from the moment of impact) points clearly to the fact that the trajectories $C_x(t)$ and $C_y(t)$ depend on the topology of the grid. The self-oscillating regime is established somewhat more rapidly on the cylindrical grid. This, probably, is

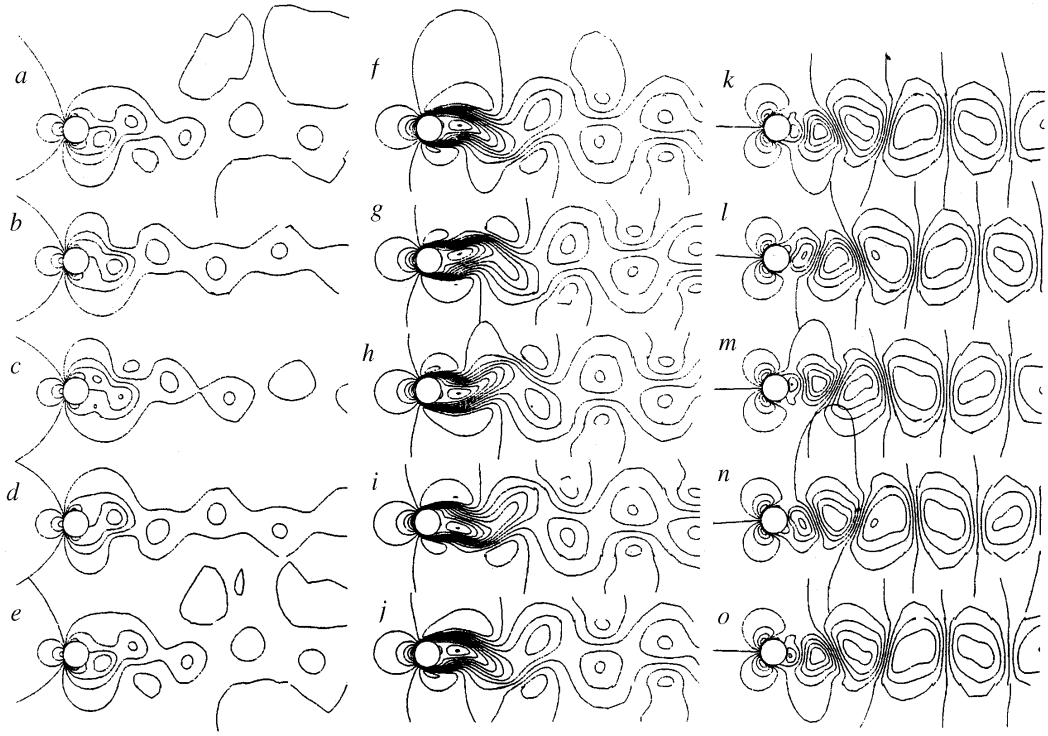

Fig. 4. Patterns of the isobars (a–e) and the isotachs of the longitudinal (f–j) and vertical (k–o) velocity components (step 0.15) in the self-oscillating regime of flow around the circular cylinder at the instants of time: t = 81.1 (a, f, k), 82.5 (b, g, l), 83.9 (c, h, m), 85.3 (d, i, n), and 86.7 (e, j, o).

explained by the scale effect, i.e., by the fact that the size of the circular region is smaller than the size of the rectangular region considered. In the first case, the disturbances from the back boundary exert a destabilizing action on the flow around the cylinder more rapidly. It should be noted that the character of the dependences $C_x(t)$ and $C_y(t)$ is analogous to the dependences obtained earlier in [8].

An analysis of nonstationary flow around a circular cylinder, carried out on a composite grid, is made in Figs. 3–7.

An analysis of the time dependences of the extreme local parameters of the flow, i.e., the minimum velocity of the reverse flow in the wake $u_{\min}$ (Fig. 3a) and the minimum pressure $p_{\min}$ (Fig. 3b), and of the evolution of the drag and lift coefficients has revealed several characteristic portions of the behavior of the parameters. Their existence has been suggested earlier [8].

First of all, we should note the phase of the beginning of the process of formation of nonstationary flow around a circular cylinder. The "impact" character determines the large initial gradients of all the dependences considered and the high rate of development of the process. It is of interest to estimate the duration of the phase relative to the duration of formation of the self-oscillating regime of flow around the cylinder. It was found that it accounts for about 3% of the indicated time interval. A detailed analysis of the initial phase has been made in [8].

Subsequently, the rate of development of the process decreases. Approximately to the instant t = 45, there is a region where the minimum velocity in the near wake behind the cylinder changes almost linearly at a practically constant static pressure. This portion with a duration of about 45% of the time of formation of the self-oscillating regime of the flow is characterized by the absence of the lift (lifting force) and a gradual decrease in the drag coefficient to its minimum value.

The next stage completing the transient process of formation of the self-oscillating regime of flow around the cylinder accounts for about 50% of the time of its establishment. This stage is characterized by a gradual decrease in the minimum pressure in the wake and an increase in the absolute value of the minimum longitudinal velocity. The oscillations of the above characteristics caused by the transverse oscillation of the flow become quite appreciable. The

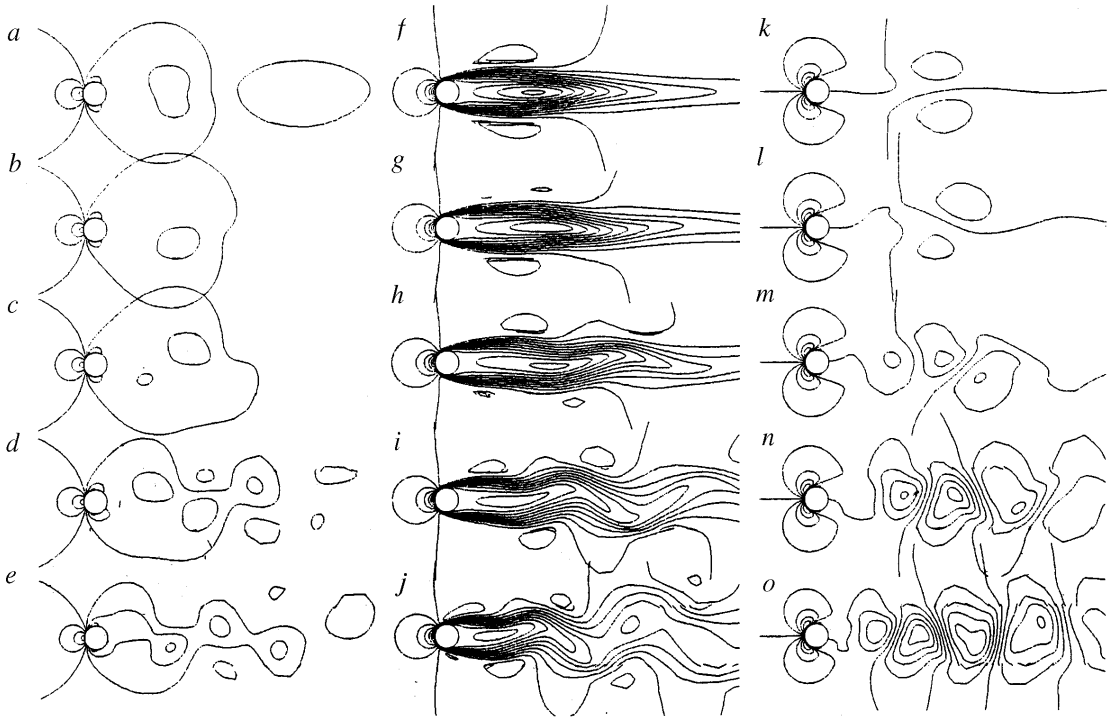

Fig. 5. Patterns of the isobars (a–e) and the isotachs of the longitudinal (f–j) and vertical (k–o) velocity components at the initial period of laminar flow around the circular cylinder at the instants of time: t = 1 (a, f, k), 5 (b, g, l), 10 (c, h, m), 15 (d, i, n), and 20 (e, j, o).

oscillations of the drag and lift coefficients also increase gradually; with increase in the oscillation amplitude the averaged drag of the cylinder also increases.

To determine the interrelation between the evolution of the local and integral characteristics of the flow and the instantaneous patterns of flow around the cylinder, by points on the dependence $C_y(t)$ (Fig. 3d) we denoted the instants of time (in the self-oscillating regime of flow) for which the patterns of the isobars and isolines of the longitudinal and transverse velocity components are constructed with a step of 0.15 (Fig. 4).

It is usual to analyze separated flow around a circular cylinder using the patterns of vorticity isolines. In the present work, increased attention is given to the study of synchronous patterns of pressure and velocity fields. Figure 4 shows the patterns in a quarter of the period; consideration begins from the instant corresponding to the minimum value of the lift coefficient.

As is seen from the isobars presented, the vortices separated alternately from the lower and upper halves of the cylinder enter successively the flow and move downstream. The centers of the vortices corresponding to the zones of decreased pressure move along parallel straight lines collinear to the velocity vector of the undisturbed flow, forming the known Karman vortex street. At the instant of vortex separation, the lift coefficient has a maximum value.

Analysis of the patterns of the isolines of the velocity components gives additional information on the generation of the vortex street. Noteworthy is the dissimilarity of the separated flow near the body from the vortex flow in the developing wake. As follows from the patterns of the isolines of the longitudinal velocity components, a flow toward the bottom part of the cylinder which is similar to the jet flow is formed in the neighborhood of the body. The maximum velocity of the reverse flow accounts for about 0.3 of the undisturbed-flow velocity. The jet beating the bottom part of the cylinder is weakly pulsating and shifts alternately up and down relative to its axial line oriented along the vector of the undisturbed flow. The character of the behavior of the isolines of the transverse velocity components also points to the fact that the back part of the cylinder is in pulsating alternating transverse flow.

The structure of the flow in the wake behind the cylinder downstream is periodic in longitudinal and transverse velocity components.

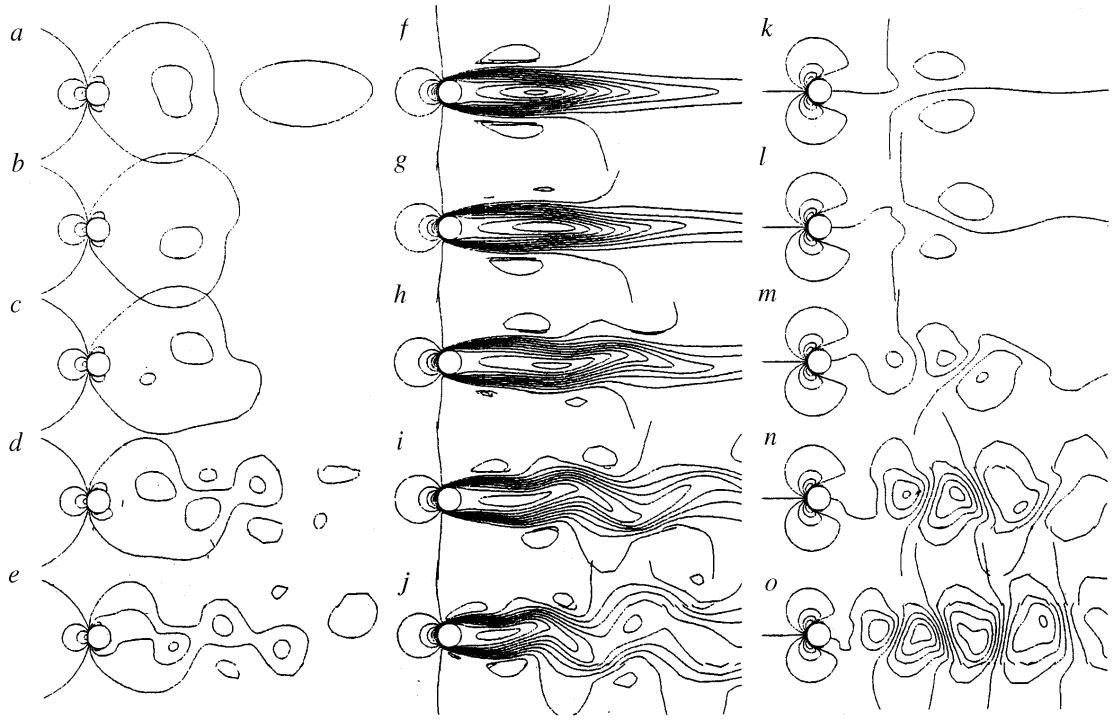

Fig. 6. Patterns of the isobars (a–e) and the isotachs of the longitudinal (f–j) and vertical (k–o) velocity components (step 0.15) in the transient regime (with asymmetrization) of flow around the circular cylinder at the instants of time: t = 25 (a, f, k), 30 (b, g, l), 35 (c, h, m), 40 (d, i, n), and 45 (e, j, o).

Figures 5–7 show the patterns of flow around the cylinder, which correspond to the initial phase and to the transient process and have been constructed with a time step close to 5. It is apparent that they correspond to the above-mentioned phases of flow around the cylinder. True enough, the initial phase of flow around the cylinder is interpreted broadly — to the instant t = 20, i.e., to the boundary of existence of the symmetric vortex structure in the wake behind the cylinder (Fig. 5). Clearly, this period involves a part of the linear portion of the dependence $u_{\min}(t)$ and, what is more important, the nonlinear portion of the dependence $p_{\min}(t)$. The considered phase of flow is distinguished by the predominance of the rapid processes of formation of the near wake, which are accompanied by a high rarefaction and high velocities of the reverse flow. As the length of the separation zone increases, the velocity of circulation flow and the level of flow pressure in it decrease. It is important to note that the length of the zone at the end of the initial phase is much larger than the diameter of the cylinder.

In the first phase of the transient process, elements of asymmetry appear in the flow as a result of the stability loss and the transformation of the vortex structure in the near wake behind the cylinder, which lasts to t = 45 (Fig. 6). The loss in the symmetry of the flow in the wake is the most pronounced in the evolution of the patterns of the isolines of the transverse velocity components. The wake changes gradually, which is evidenced by the monotonic character of the dependences $u_{\min}(t)$ and $p_{\min}(t)$. Whereas $u_{\min}(t)$ behaves linearly, $p_{\min}(t)$ changes very insignificantly. Such behavior of the local characteristics of the flow is due to the fact that in the time interval considered all the changes occur at a small distance from the cylinder. It is of interest to note that at the end of the period the vortex structure in the far wake is topologically similar to the structures of the self-oscillating regime. By this instant the length of the separation zone in the near wake behind the cylinder also decreases markedly. It should be emphasized that the fluid motion before the cylinder is still symmetric. As a consequence, the lift coefficient of the cylinder remain neglectfully small, i.e., the distributions of the pressure and the friction over its surface differ insignificantly from symmetric distributions.

The second stage of the transient process (Fig. 7) is characterized by the development of nonstationary flow around both the front and back halves of the cylinder. Its duration varies from 50 to 80. At this stage of flow, the

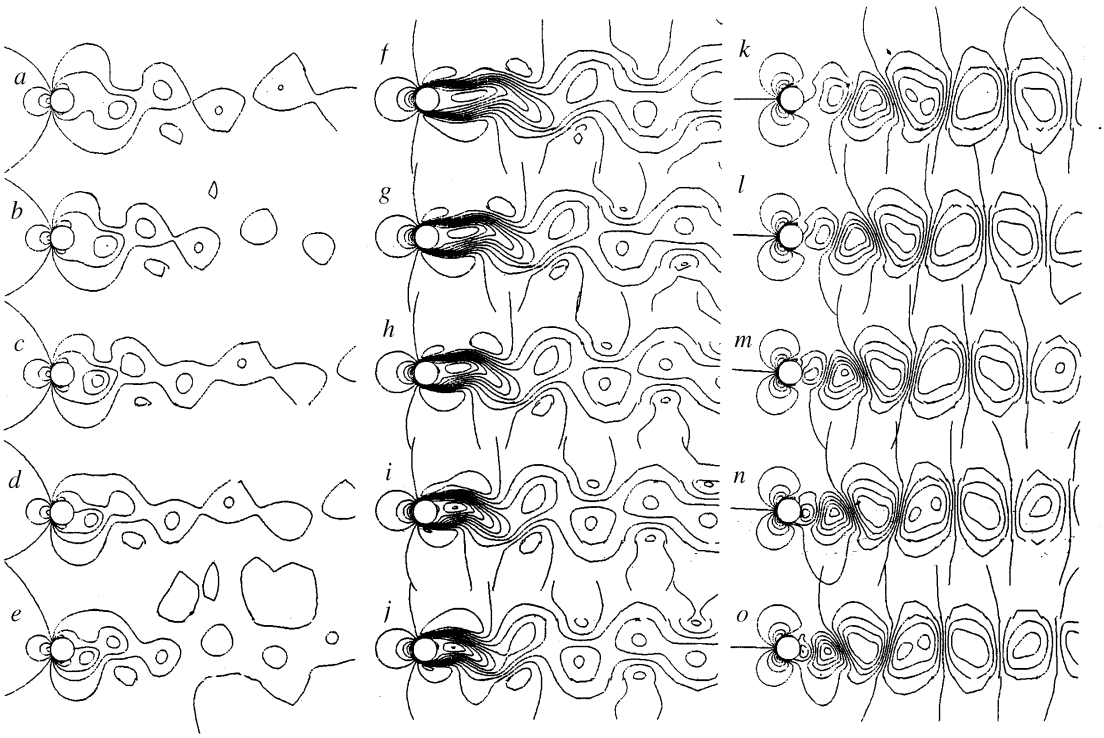

Fig. 7. Patterns of the isobars (a–e) and the isotachs of the longitudinal (f–j) and vertical (k–o) velocity components (step 0.15) in the transient regime of flow around the circular cylinder at the instants of time: t = 50 (a, f, k), 55 (b, g, l), 60 (c, h, m), 65 (d, i, n), and 70 (e, j, o).

TABLE 1. Comparison of the Calculated and Experimental Results on the Strouhal Number for Laminar Flow around the Circular Cylinder at Re = 150

Literature source	Present work	[8]	[14]	[15]	[16]	[17]
Strouhal number	0.182	0.18	0.182	0.182	0.183	0.185

cylinder is found in the flow with a variable angle of attack. As a consequence, the integral loads on the body increase, and the rarefaction and the velocity of the reverse flow in the near layer increase.

A comparison of the calculated and experimental values of the Strouhal number, obtained with different computational grids and in experiments on different setups [14–17] in the self-oscillating regime of the flow around the circular cylinder at Re = 150, has shown that they are in good agreement.

The dependence of the Strouhal number on the time, beginning with the instant of sudden motion of the flow, correlates with the above-described phases of flow around the cylinder (Fig. 3c). The initial portion is characterized by an abrupt decrease in Sh, and the initial phase of the symmetric flow and the region of the transient process with elements of flow asymmetry is characterized by a constant level of Sh. From the second phase of the transient process, Sh begins to increase gradually to the values obtained in the experiments.

This work was carried out with financial support from the Russian Foundation for Basic Research (project Nos. 02-02-81035, 02-01-00670, and 02-01-01160).

NOTATION

t, time; R_1, distance to the boundary of the computational region; $u_{\min}$ and $p_{\min}$, minimum values of the longitudinal velocity component and the static pressure; Re and Sh, Reynolds and Strouhal numbers; C_x and C_y, coefficients of drag and of transverse force.

REFERENCES

1. J. E. Fromm, *Meth. Comput. Phys.*, **3**, 345–382 (1964).
2. S. A. Isaev, A. G. Sudakov, N. N. Luchko, and T. V. Sidorovich, *Inzh.-Fiz. Zh.*, **75**, No. 1, 54–60 (2002).
3. I. A. Belov and N. A. Kudryavtsev, *Heat Transfer and Resistance of Tube Piles* [in Russian], Leningrad (1987).
4. I. A. Belov, S. A. Isaev, and V. A. Korobkov, *Problems and Methods of Calculation of Separating Flows of Incompressible Fluids* [in Russian], Lenigrad (1989).
5. J. H. Ferziger and M. Peric, *Computational Methods for Fluid Dynamics*, Berlin (1999).
6. P. A. Baranov, S. A. Isaev, Yu. S. Prigorodov, and A. G. Sudakov, *Pis'ma Zh. Tekh. Fiz.*, **24**, Issue 8, 33–41 (1998).
7. P. A. Baranov, S. A. Isaev, Yu. S. Prigorodov, and A. G. Sudakov, *Izv. Vyssh. Uchebn. Zaved., Aviats. Tekh.*, No. 3, 30–35 (1999).
8. P. A. Baranov, S. A. Isaev, and A. G. Sudakov, *Izv. Ross. Akad. Nauk, Mekh. Zhidk. Gaza*, No. 2, 68–74 (2000).
9. P. A. Baranov, S. A. Isaev, and A. E. Usachev, *Inzh.-Fiz. Zh.*, **73**, No. 3, 606–613 (2000).
10. V. L. Zhdanov, S. A. Isaev, and Kh. Yu. Nimann, *Inzh.-Fiz. Zh.*, **74**, No. 5, 36–38 (2001).
11. S. A. Isaev, A. G. Sudakov, P. A. Baranov, and N. A. Kudryavtsev, *Inzh.-Fiz. Zh.*, **75**, No. 2, 28–35 (2002).
12. D. Barkley and R. Henderson, *J. Fluid Mech.*, **322**, 215–241 (1996).
13. S. H. K. Williamson, *J. Fluid Mech.*, **328**, 345–407 (1996).
14. S. H. K. Williamson and A. Roshko, *Z. Flugwissund. Weltraumforsch.*, **14**, Nos. 1–2, 38–46 (1990).
15. S. H. K. Williamson and A. Roshko, *J. Fluid Mech.*, **206**, 579–627 (1989).
16. C. Norberg, *J. Fluid Mech.*, **258**, 287–316 (1994).
17. B.-K. Min and K.-S. Chang, *Int. J. Numer. Meth. Fluids*, **28**, No. 3, 443–460 (1998).